Journal of Materials Chemistry A

PAPER

Cite this: J. Mater. Chem. A, 2017, 5, 3503

Defect interactions and the role of complexes in the CdTe solar cell absorber

Dmitry Krasikov* and Igor Sankin

Received 21st October 2016
Accepted 13th January 2017

DOI: 10.1039/c6ta09155e

www.rsc.org/MaterialsA

While the electrical and optical properties of most crystalline materials are determined by the point defects, the association of these defects into complexes may further alter material properties, introducing new important phenomena. The properties of isolated point defects in CdTe have attracted significant research efforts, yet understanding of the complex defects in this material remains insufficient. This paper investigates the thermodynamic aspects of defect association in chlorinated copper-doped CdTe absorbers from first principles, using a supercell approach with the range-separated hybrid exchange–correlation functional. Based on the complex association energies calculated for 76 defect reactions, we propose the most favorable pair complexes formed in Cl- and Cu-doped CdTe absorbers. Most of the complexes studied in this work appear to be harmful for p-doping and may be responsible for the performance instabilities observed in CdTe devices. We also discuss a plausible passivation mechanism that mitigates Te_{Cd} recombination centers during Cl treatment and consider the formation of larger defect clusters and segregation of the point defects on extended defects.

1. Introduction

The efficiency of CdTe-based solar cells depends to a large degree on the electric properties of the CdTe absorber layer, which, in turn, heavily depend on the amount and properties of the electrically active centres (crystalline defects) in it. The record efficiency of CdTe-based thin-film solar cells has recently reached 22.1%.[1] This impressive result, however, is still far from the theoretical maximum (~30%), leaving appreciable room for improvements. In particular, the formation of a stronger p-type absorber doping and the mitigation of absorber recombination centres to achieve longer carrier lifetime could further improve the open-circuit voltage.[2] As an additional and important requirement, the concentration and distribution of crystalline defects in the absorber should remain constant under field stress conditions to ensure stable device performance.

The typical fabrication process of a CdTe PV device includes a high-temperature annealing step at 400–450 °C in the presence of chlorine and a p-type doping formation step at 200–300 °C to introduce and activate Cu acceptors. Chlorine and copper introduced to CdTe at concentrations[3–6] of 10^{17} to 10^{19} cm^{-3} form point defects that strongly affect the electrical performance of the absorber. Recently, the properties of Cu- and Cl-related point defects in CdTe absorber became a subject of intensive research.[7–12] At the same time, the defect complexes consisting of more than one point defect have attracted much less attention, and their role in the formation of doping and recombination centres remains unclear. In this work, we analyse the interactions of major point defects causing the formation of defect complexes and discuss the impact of resulting complexes on the doping, recombination properties, and stability of CdTe absorbers.

We base our work on the series of preceding studies[9–25] that systematically analysed the structure and electric properties of intrinsic and Cu- and Cl-related point defects in CdTe. The electric character of the point defects derived using the first-principles calculations is in agreement with the experimental data (Grill *et al.*[18,19]) and can be summarized as follows. The cadmium vacancy V_{Cd} is a non-shallow double acceptor. The cadmium antisite Cd_{Te}, the tellurium vacancy V_{Te} and the interstitial cadmium Cd_i are shallow double donors. The interstitial tellurium Te_i and tellurium antisite Te_{Cd} are deep double donors. The substitutional copper Cu_{Cd} is a non-shallow acceptor, while the interstitial copper Cu_i and the chlorine on tellurium site Cl_{Te} are shallow donors. The interstitial chlorine Cl_i may act as a donor or an acceptor depending on its position in the CdTe lattice.[10,21] Although no study on the recombination activity of Cl- and Cu-related defects in CdTe is reported to date, certain attempts were made to theoretically analyse the recombination properties of intrinsic defects. According to the analysis of multiphonon carrier capture rates, Te_{Cd} is the most active recombination centre among the intrinsic defects in CdTe.[24,25]

Compared to the point defects, there have only been scattered efforts to investigate the complex defects in CdTe.[10,11,17,20,26] Below, we summarize the major findings of these studies. (Cu_i–Cu_{Cd}) is a deep donor complex that can diffuse, and (Cl_{Te}–V_{Cd}) is an acceptor complex with ionization

First Solar Inc., 28101 Cedar Park Blvd, Perrysburg, OH 43551, USA. E-mail: dmitry.krasikov@firstsolar.com; igor.sankin@firstsolar.com

This journal is © The Royal Society of Chemistry 2017

level at 0.1–0.22 eV from the valence band maximum (VBM). (V_{Cd}–Te_{Cd}) is a deep double acceptor complex with (0/−2) ionization level located at ~1.0 eV from VBM, and (Te_i–Te_{Cd}) complex has a binding energy of −1.2 eV, while the (Te_i–Te_i) complex is weakly bound. The cadmium vacancy V_{Cd} does not form complexes with other cation and anion vacancies.

Multiple studies have investigated the impact caused by complex defects on the macroscopic properties in different materials. Examples include doping compensation by the association of dopants with intrinsic defects (see *e.g.* ref. 27 and 28) and aging of ferroelectrics due to the reorientation of dipoles formed by complex defects.[29] Other examples include the appearance of yellow luminescence in GaN,[30] the high rate of non-radiative recombination in InGaN alloys,[31] and light-induced metastabilities in Cu(In, Ga)Se_2 solar cells.[32–34] Passivation of impurities in Si by hydrogen[35] and retention of the hydrogen in metals[35,36] provide another set of examples. Together with a general assumption of the detrimental role of complexes in semiconductor devices,[37] this list emphasizes the need to improve the understanding of defect complexes in CdTe absorbers and their effect on the electronic properties and stability.

The instability of electronic properties of CdTe-based PV devices is another long-standing issue[38] that has attracted considerable research interest.[39–47] Several studies have attributed metastabilities to Cu redistribution in the device.[8,48–50] At the same time, Gretener *et al.*[42] reported the instabilities in CdTe solar cells observed even without noticeable Cu redistribution. Guillemoles *et al.* proposed so-called short-range effects not involving the long-range diffusion of species to explain metastabilities observed in CIGS PV cells.[51] Such effects include relatively fast transition of a defect or a complex into the metastable state and defect reactions. To our knowledge, the role of short-range effects in CdTe solar cells is still unclear.

Section 2 of this work lists the assumptions and provides details on the methods used in this study. In Section 3, we report the energies of pair interactions between the major point defects in Cl- and Cu-treated CdTe absorbers obtained from the calculated enthalpies of defect reaction and ionization levels of defects and complexes. In sub-section 4.1, we derive a quantitative association criterion used to evaluate the association probability of the defects during Cl and Cu treatments and determine the most favourable pair complexes. In the following sub-section 4.2, we discuss the impact of defect association on p-type doping in the CdTe absorber. Sub-section 4.3 discusses the possibility of passivation of the Te_{Cd} recombination centre by Cl, and sub-section 4.4 discusses the potential mechanisms of instabilities induced by pair complexes in Cl- and Cu-treated CdTe absorbers. Finally, in sub-section 4.5, we discuss the processes that may potentially limit the applicability of the model of pair complex formation, *i.e.* the association of point defects into larger defect clusters and the segregation on extended defects.

2. Methodology

2.1 Assumptions

2.1.1 Primary defects. We consider four intrinsic point defects (Cd_i, V_{Cd}, Te_i, Te_{Cd}) and four point defects formed by chlorine and copper (Cl_i, Cl_{Te}, Cu_i, Cu_{Cd}). Since the formation of Cd_{Te} and V_{Te} requires a long equilibration in a Te-poor environment not found in standard processing, we exclude these defects from consideration. Even if formed in some amount, they convert into Cl_{Te} defects in the chlorinated CdTe, according to the calculated formation energies.[10,14] As we consider the species in the different charge states, we deal with 12 different point defects: Cd_i^{2+}, V_{Cd}^{2-}, Te_i^0, Te_i^{2+}, Te_{Cd}^0, Te_{Cd}^{2+}, Cl_i^+, Cl_i^-, Cl_{Te}^+, Cu_i^+, Cu_{Cd}^0, and Cu_{Cd}^- participating in 78 reactions, including the reaction with the same kind of defect.

2.1.2 Excluded reactions. We do not consider reactions between V_{Cd} and Cu_{Cd}. These species do not coexist, because Cu_i and Cd_i fill all the residual V_{Cd}, while the Cu annealing temperature is too low to form new cadmium vacancies or diffuse existing vacancies from the interfaces. This leaves 76 reactions in total.

2.1.3 Defect chemistry. Any defect reaction consists of forward and backward reactions described by rate constants linked through the equilibrium constant. The equilibrium constant defined by the reaction energy and temperature determines the direction of a reaction and the equilibrium concentrations of reactants and products. In this work, we primarily analyse the equilibrium constants of defect reactions.

2.1.4 Bimolecular defect reactions. We only consider bimolecular reactions where two well-separated, non-interacting point defects merge into a product (single point defect or complex). In the following discussion, the reactions that proceed from the left to the right are called "forward", and the reactions from the right to the left are called "backward". This description covers three types of possible defect reactions:

• The association/dissociation of a complex,

$$\text{Defect}_1 + \text{defect}_2 \overset{\Delta E}{\rightleftharpoons} \text{complex defect} \quad (1)$$

• The exchange reactions facilitated by kick-out,

$$A_i + B_A \overset{\Delta E}{\rightleftharpoons} B_i \quad (2)$$

In the forward exchange reaction, a self-interstitial defect A_i kicks out a substitutional defect B_A formed by an element B on the lattice site belonging to an element A in a regular lattice. This exchange reaction forms a regular lattice site A_A and an interstitial defect B_i. In the backward reaction, B_i replaces A on its regular site, forming B_A and a mobile interstitial A_i that diffuses away from the reaction site.

• The formation/recombination of a vacancy and an interstitial defect,

$$B_i + V_A \overset{\Delta E}{\rightleftharpoons} B_A \quad (3)$$

In the recombination reaction (forward direction), an interstitial defect comes close to a vacancy and falls into it, which is usually energetically favourable. The backward reaction is the jump-out of an atom from a substitution lattice site into an interstitial site and the separation of thus-formed interstitial

 This journal is © The Royal Society of Chemistry 2017

defect and a vacancy. If a regular lattice atom jumps out, then a Frenkel pair forms in such a backward reaction.

2.1.5 Theoretical energy of reaction. We estimate the energy change in the above-mentioned reactions as a difference between formation enthalpies of products and reactants obtained from first-principles calculations using large supercells and the range-separated hybrid functional.

2.2 Reaction energies and ionization levels

We can express all three types of reactions discussed in Section 2.1 in a more general form,

$$R_1 + R_2 \rightleftharpoons^{\Delta H} P, \quad (4)$$

where R_1 and R_2 are reactants, and P is a product that could be a complex, an interstitial, a substitutional defect or a regular lattice site for the reactions described by eqn (1)–(3), respectively. The enthalpy change in the forward reaction is

$$\Delta H = H_f(P) - H_f(R_1) - H_f(R_2). \quad (5)$$

In eqn (5), $H_f(S)$ represents the formation enthalpy of a corresponding species. Since all the considered reactions conserve both the mass and the charge, the final expression for the reaction enthalpy does not contain the enthalpies of species in their reference states. In the supercell approximation, the reaction enthalpy reads as follows:

$$\Delta H = E(P) + E(\text{Bulk}) - E(R_1) - E(R_2) + (q_1 + q_2)\Delta V(P) - q_1\Delta V(R_1) - q_2\Delta V(R_2) \quad (6)$$

The total energy of the ideal defect-free supercell is given by E(Bulk), while E(S) is the total energy of a supercell containing a corresponding species that carries a charge q. Here, we count the valence band minimum (VBM) correction ΔV based on the average potential far from a defect.[52] To calculate the total energies, we need to know the most favourable atomic structure of defects and complexes in each charge state. While we obtain such structures for point defects from previous works, we still need to calculate them for the complex defects. To do this, we build different atomic configurations of a complex by placing two point defects on the possible adjacent lattice sites known from the studies of point defects, and then we optimize these configurations under GGA-PBE approximation by minimizing the energy down to 0.02 eV Å^{-1}. After optimization, we calculate the total energies of relaxed structures using HSE06 hybrid functional and choose the structures with the lowest energies. In all calculations, we use the large 216-atom cubic GGA-PBE-optimized CdTe supercells with the size of 19.83 Å. Although this supercell size does not fully resemble the physical problem with the well-separated point defects, it provides enough space to recover the macroscopic bulk behaviour for electrostatic screening and elasticity between the defects or complexes in the neighbouring images and to minimize the overlap of defect wave functions.

To calculate thermodynamic ionization levels of the complex defects, we use the formula:

$$\varepsilon_{th}(q/q') = \frac{E_q(Q_q) - E_{q'}(Q_{q'})}{q' - q} - \varepsilon_{VBM}^{Bulk} + \frac{q\Delta V - q'\Delta V'}{q' - q}, \quad (7)$$

where q and q' are the charges carried by a complex in corresponding charge states, $E_q(Q_q)$ is the total energy of a supercell with charge q in the most stable atomic configuration Q_q for this charge state, ε_{VBM}^{Bulk} is the VBM energy of bulk CdTe, and ΔV is the VBM correction for a defective supercell in the corresponding charge state.

In some cases, the charge of the product in its most favourable state differs from the sum of the charges carried by the reactants, meaning that the product traps or releases a free carrier after its formation. We obtain the total energy of such an "extended" reaction as a sum of the reaction enthalpy (eqn (6)) and the energy of carrier transition from the corresponding reservoir into the unoccupied defect levels. For example, the energy required to move an electron described by the Fermi level μ_F from the reservoir into an unoccupied defect level is $\varepsilon_{th}(q/q') - \mu_F$.[53] Therefore, the overall energy of the reaction with the change of the charge state is

$$\Delta E = \Delta H + (q_1 + q_2 - q_P)\cdot(\varepsilon_{th}((q_1 + q_2)/q_P) - \mu_F). \quad (8)$$

In eqn (8), $\varepsilon_{th}((q_1 + q_2)/q_P)$ represents the ionization level of a product species determined using eqn (7), and q_P is the most favourable charge state of a product for a given Fermi level.

2.3 Computational tools

We perform all calculations using the *ab initio* total-energy and molecular-dynamics package VASP (Vienna ab initio simulation package) developed at the Institut für Materialphysik of the Universität Wien[54] and integrated into the MedeA® software environment.[55] In all calculations, we use plane wave basis set with 300 eV energy cut-off together with the projector augmented wave (PAW) potentials,[56,57] describing the interactions of valence electrons with core states. We use the generalized gradient approximation (GGA) to the density functional theory parametrized by Perdew–Burke–Ernzerhof (PBE) to optimize the structures.[58] For the total energy calculations, we use HSE06 (ref. 59) range-separated exchange–correlation hybrid functional with default parameters. Most of the calculations are performed using computational resources of the Ohio Supercomputer Centre (Columbus, Ohio, USA).

3. Results

To calculate the enthalpies of the reactions, we identify the most stable products considering different reaction pathways. By comparing results, we find that the interstitial–vacancy complexes, *e.g.* $(Cu_i–V_{Cd})^-$, are not stable and tend to convert into substitution defects. Similarly, the complex of self-interstitial with substitution defect is not stable and converts into an interstitial defect by kick-out reaction. For example, the reaction $Cd_i^{2+} + Cu_{Cd}^-$ tends to produce interstitial copper Cu_i^+ rather than the $(Cd_i–Cu_{Cd})^+$ complex. Of 76 total reactions, there are 66 reactions of complex formation, with only three exchange

reactions and six reactions of vacancy–interstitial recombination.

Table 1 summarizes the enthalpies of reactions resulting in the most energetically favourable products. All the exchange reactions and majority of the vacancy–interstitial recombination and complex formation reactions have negative reaction enthalpy. Despite the common perception that only donor–acceptor association is possible, we find that some of the donor–donor association reactions have negative binding enthalpies (*e.g.* Cl_i^+ with Cl_i^+, Cl_i^+ with Te_{Cd}^{2+} *etc.*).

We further use the calculated association enthalpies to derive the energies of association reactions with the change of charge state using eqn (8). By comparing different possible association reactions for each point defect, we have chosen nine most favourable complexes with the lowest association energies in the whole range of Fermi levels.

Fig. 1 presents the most favourable atomic structures of these primary complexes. We find that for some complexes, such as $(Cu_i–Cu_{Cd})^+$ and $(Cl_i–Cl_i)^{2-}$, the atomic structure resembles the structure of constituting defects placed nearby, while for the other complexes, it is not the case. We also find that different complexes behave differently upon the change of the charge state. For most of the complexes, we do not observe any significant change of the atomic structure after recharge except some variation of bond lengths. For three complexes, namely, $(Cl_i–Cl_i)$, $(Cl_i–Cu_{Cd})$, and $(Te_i–Cu_{Cd})$, we find different local energy minima for different charge states and strong lattice relaxation (change of the atomic configuration) resulting from the change of the charge state. This may cause additional effects, as we will discuss further.

Fig. 2 summarises the ionization levels of all the primary complexes. All these levels are either of the donor character or of the deep acceptor character. Therefore, we conclude that in p-type CdTe, all complexes behave as donors or neutral defects.

The energies of the association reactions for the primary complexes are plotted in Fig. 3. These energies are grouped into three types, according to defects: the association of Cl_i, the association of Te_i, and the association of the residual Cu_{Cd} remaining after association with Cl_i or Te_i. Most of the primary complexes have Fermi level-dependent association energies in a certain range of Fermi levels, which indicate the association with the change of the charge state.

4. Discussion

4.1 The association criterion

Given the defect formation energy E_f as well as the concentration of available lattice sites N_{sites} and the number of possible configurations N_{config} for an arbitrary defect species, its equilibrium concentration could be calculated using Boltzmann approximation for diluted concentrations as[60]

Table 1 The calculated enthalpies of the reactions between all point defects under consideration. Integer numbers depict the type of each reaction: 1 – complex formation, 2 – exchange reaction facilitated by kick out, 3 – vacancy–interstitial pair annihilation

	Cl_i^-		Cl_i^+		Cl_{Te}^+		Te_i^0		Te_i^{2+}		Te_{Cd}^0		Te_{Cd}^{2+}		Cu_i^+		Cu_{Cd}^0		Cu_{Cd}^-		Cd_i^{2+}		V_{Cd}^{2-}	
Cl_i^-	−0.04	1																						
Cl_i^+	−0.82	1	−0.72	1																				
Cl_{Te}^+	−1.02	1	+0.37	1	+0.02	1																		
Te_i^0	−0.58	1	+1.07	1	−0.65	2	+0.44	1																
Te_i^{2+}	+0.49	1	−0.46	1	+0.32	1	−1.42	1	−0.85	1														
Te_{Cd}^0	−0.24	1	−1.46	1	−0.44	1	−1.45	1	−1.49	1	0.54	1												
Te_{Cd}^{2+}	−1.88	1	−0.88	1	+0.16	1	−1.23	1	−0.68	1	−0.79	1	−0.03	1										
Cu_i^+	−0.04	1	−0.33	1	+0.01	1	−0.47	1	−0.11	1	−0.57	1	+0.05	1	+0.16	1								
Cu_{Cd}^0	−0.58	1	−0.48	1	−0.41	1	−0.65	1	−1.09	1	−0.72	1	−0.68	1	−0.40	1	−0.23	1						
Cu_{Cd}^-	+0.62	1	−0.65	1	−0.52	1	−0.20	1	−1.31	1	−0.04	1	−0.74	1	−0.37	1	−0.22	1	−0.07	1				
Cd_i^{2+}	+1.08	1	−0.14	1	+0.04	1	−0.54	1	+0.12	1	−0.48	2	+0.58	1	+0.02	1	−0.33	1	−1.00	2	+0.02	1		
V_{Cd}^{2-}	+0.56	3	−0.63	3	−0.74	1	−0.26	3	−2.12	3	0.33	1	−0.47	1	−1.50	3	N/A		N/A		−2.60	3	+0.55	1

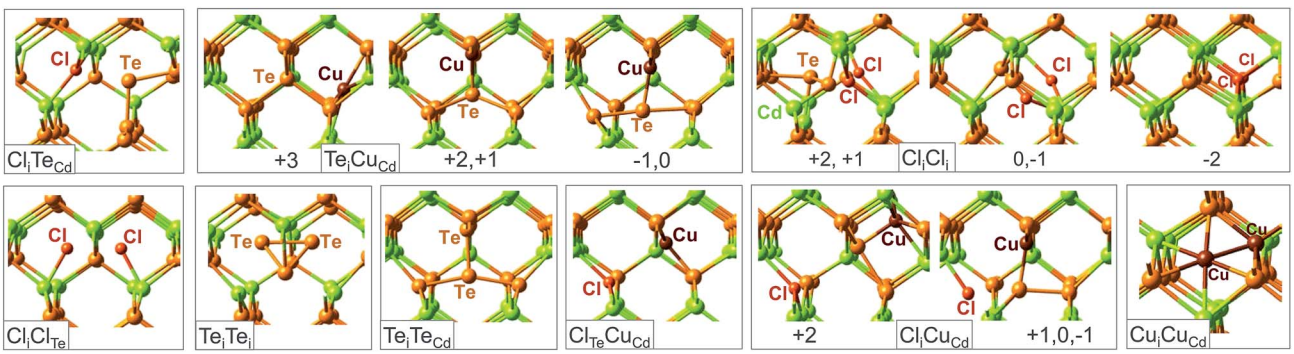

Fig. 1 Atomic structure of the most favourable complex defects in chlorinated Cu-doped CdTe absorbers.

This journal is © The Royal Society of Chemistry 2017

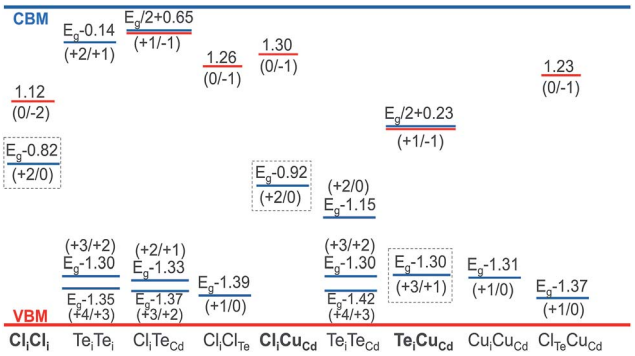

Fig. 2 The ionization levels of the most favourable complexes with respect to VBM. The double lines indicate the amphoteric (donor–acceptor) levels. The complexes with strong atomic configuration changes are marked in bold, and the dashed rectangles indicate the corresponding ionization levels.

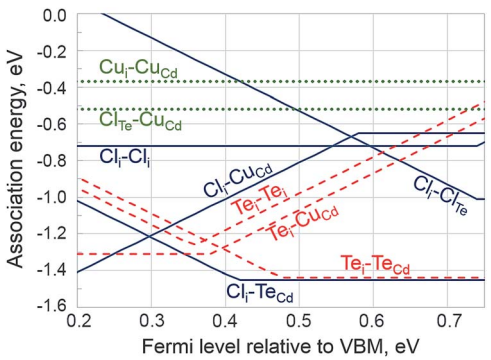

Fig. 3 The association energies of the most favourable complexes in the intrinsic and p-type CdTe. The horizontal lines indicate defect association without the change of charge state; the inclined lines indicate association with the change of charge state.

$$c = N_{\text{sites}} N_{\text{config}} \exp\left(-\frac{E_f}{kT}\right). \quad (9)$$

Let us define the density of its available microstates as $N_{\text{states}} = N_{\text{sites}} N_{\text{config}}$. Then, assuming approximately equal concentrations of available microstates N_{states} for the reactants and the product, we can use the law of mass action to estimate equilibrium concentration of a complex product as

$$C_{AB} = \frac{C_A C_B}{N_{\text{states}}} \exp\left(-\frac{\Delta E}{kT}\right). \quad (10)$$

In eqn (10), C_A and C_B are the concentrations of isolated point defects A and B, respectively, C_{AB} is the concentration of complex defect AB, and the association energy ΔE is obtained from Fig. 3. Note that such formulation is applicable to a general case of association accompanied by the change of charge state. If the energy ΔE depends on the Fermi level and changes during the association, then finding the equilibrium concentration C_{AB} would require a self-consistent solution to the defect chemistry problem.

To assess the probability of defect association at different stages of solar cell preparation, we introduce a qualitative criterion of association degree. Let us select A and B such that $C_B \gg C_A$, where C_A and C_B could be either equilibrium or kinetically constrained concentrations of defects. Then, we can define the association degree as a concentration ratio between the complex and the minority defect C_{AB}/C_A.

In the case of high association degree when $C_{AB} \geq C_A$, the association energy should satisfy the condition

$$\Delta E \leq -kT \log\left(\frac{N_{\text{states}}}{C_B}\right). \quad (11)$$

Note that in the approximation of diluted concentrations when $C_B \ll N_{\text{states}}$, condition (11) requires negative ΔE. We introduce the critical association energy $\Delta E_{\text{crit}} = kT \log(N_{\text{states}}/C_B)$ so that

$$|\Delta E| \leq \Delta E_{\text{crit}}. \quad (12)$$

When the absolute value of the association energy exceeds ΔE_{crit}, more than half of the minority defects are associated into complexes. In the estimates shown in Fig. 4, we use N_{states} equals the density of lattice sites in CdTe.

From Fig. 4, we see that as the temperature decreases, the association degree increases for a given value of ΔE_{crit}. A practical take-away from this observation is that interstitial defects not bound in complexes during high-temperature processing would tend to form complexes on cool-down. The calculated diffusivities[11,12,17,61,62] of Cu_i^+, Cd_i^{2+}, Te_i^{2+} and Cl_i^+ interstitial defects in CdTe are in the range of 10^{-14} to 7×10^{-10} cm^2 s^{-1} at room temperature, which is sufficient to pass the mean distance between defects with concentrations of 10^{16} to 10^{17} cm^{-3} within minutes or faster. Therefore, during or after cooling down to room temperature, most of the remaining interstitial defects in p-type CdTe will tend to react with other defects. Depending on the conditions and parameters of the reactions, this will lead to formation of complexes, kicking out foreign atoms from their native lattice sites (*e.g.*

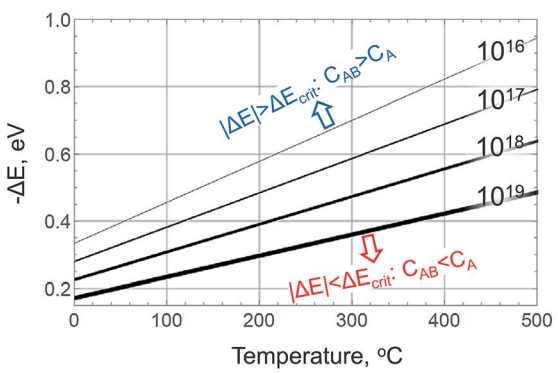

Fig. 4 Dependence of ΔE_{crit} on the temperature and the concentration of majority defect C_B calculated for $N_{\text{states}} = 1.48 \times 10^{22}$ cm^{-3}. Solid lines of different thicknesses show ΔE_{crit} for four different C_B concentrations.

Te_i will knock out Cl_{Te}; Cd_i will kick out Cu_{Cd}; *etc.*) or to recombination with the vacancies.

Fig. 4 also shows that, at a fixed temperature, the association degree increases at higher concentrations of a majority defect C_B. Given as an example, for $T = 400$ °C and $\Delta E = -0.7$ eV, the association degree would be very low (<11%) in the case of $C_B = 10^{16}$ cm^{-3}, while becoming very significant (>92%) in the case of $C_B = 10^{19}$ cm^{-3}.

4.2 The doping

In this section, we discuss the impact of complexes on p-type doping in CdTe absorbers. After a general discussion of the impact of defect association on the doping level, we consider specific cases linked to Cl treatment and Cu doping stages. In the following discussion, we assume that free charge carriers are in thermal equilibrium and, therefore, omit the possible effects of photo-generated carriers on the defect formation energies discussed by Alberi and Scarpulla.[63]

As the doping depends on the balance between the charged acceptors and donors, our goal is to reveal how the formation of complexes may affect this balance. Here, we consider two cases when the complex formation occurs with and without change in the charge state.

4.2.1 The association without the change of the charge state. In a closed system, association of the compensating defect into a complex with charge conservation does not influence the net doping. However, if there is an external reservoir that can re-supply compensating defect species to the system, association of such a defect into a complex will lead to doping reduction. This consumption–refilling process effectively increases the solubility of compensating point defects. One may consider this as a local reduction of the formation energy of a compensating defect at the site of a complex defect. Because of the increased solubility, the system may either come to the donor–acceptor compensation regime or, being already in this regime, further reduce the uncompensated charged dopant density, which eventually results in the lower doping after cool-down.[64] A well-known example of such association is the association of dopants with intrinsic defects.[27] As discussed earlier, the association degree increases on the cool-down; however, the doping does not change if point defects do not form.

4.2.2 The association with the change of the charge state. This association directly changes the concentration of free carriers because the complex captures or releases free carriers upon association. All the inclined lines in Fig. 3 denote the association with the change of charge state; however, such association may influence the doping in different ways. If the association energy decreases with the reduction of Fermi level, as for example happens to the (Cl_i–Cu_{Cd}) complex (Fig. 3), it means that the complex becomes more stable by trapping holes from VBM. Therefore, the formation of such complex in significant quantities may reduce the net p-type doping concentration and *vice versa*. The complexes that have higher association energy at low Fermi level, such as (Cl_i–Cl_{Te}), influence the doping in the opposite way—the association is beneficial for p-type doping, while the dissociation is detrimental. Since the association energy is determined by the Fermi level and, therefore, changes during the association, the association–compensation process becomes self-balancing.

Now that we have summarized two distinct effects of defect association on doping, we analyse the doping formation during Cl- and Cu-treatment stages.

4.2.3 The doping in CdTe during the Cl-treatment stage. At this stage, the chlorine penetrates into CdTe film and mostly segregates at grain boundaries, while only a small percentage ($\sim 5 \times 10^{16}$ to 4×10^{17} cm^{-3}) penetrates the grain interior.[6,65] Inside the grain, chlorine may form not only Cl_i interstitial defects, but also Cl_{Te} and Te_i defects by kicking out Te atoms from their lattice sites. Both the interstitial Cl_i and Te_i would bind to neutral Te^0_{Cd} antisite defects formed during the non-equilibrium initial CdTe deposition stage. Created (Cl_i–Te_{Cd}) and (Te_i–Te_{Cd}) complexes are the most stable ones in CdTe before the introduction of Cu doping, which implies that all available Te_{Cd} defects will be associated into complexes. In fact, Te^0_{Cd} will be mostly bound to Cl_i because it is more energetically efficient than producing a Te_i defect. Since this association occurs without change of the charge state, it does not influence the doping.

Cl treatment usually happens in undoped CdTe absorbers before Cu introduction, so a significant percentage of interstitial Cl_i defects exists in the acceptor state. Negatively charged Cl interstitials, Cl_i^-, associate readily with the Cl_{Te}^+ or Cl_i^+ donors, forming neutral (Cl_i–Cl_{Te}) and (Cl_i–Cl_i) complexes with no change in doping concentration. Therefore, the amphoteric nature of the chlorine interstitials[10,21] and the formation of neutral Cl complexes explain why chlorine treatment does not introduce any doping to the CdTe absorber. During the cool-down after the Cl treatment stage, all the available Cl_i defects will be bound into the (Cl_i–Cl_{Te}), (Cl_i–Te_{Cd}) or (Cl_i–Cl_i) complexes.

4.2.4 The doping in CdTe during the Cu-doping stage. During the copper doping stage, Cu penetrates into CdTe and forms the Cu_{Cd}^- defects, producing p-type doping. Strong compensation of Cu doping observed in most cases happens due to a variety of donor defects that include the remaining Cu_i^+ reactants and the Cd_i^{2+} products as well as defect complexes.

Let us consider the complexes that can form at this stage. The complex with the lowest association energy in Fig. 3 is (Te_i–Cu_{Cd}). However, its formation depends on the availability of Te_i, the production of which would cost an additional 0.67 eV (Table 1). At the same time, a sufficient supply of Cl_i exists due to dissociation of (Cl_i–Cl_i) and (Cl_i–Cl_{Te}), which are less stable than (Cl_i–Cu_{Cd}). This means it is more energetically favourable to form (Cl_i–Cu_{Cd}) instead of kicking out Te_i and forming (Te_i–Cu_{Cd}). Upon its formation in p-type CdTe, (Cl_i–Cu_{Cd}) traps two holes, becoming $(Cl_i–Cu_{Cd})^{2+}$ and resulting in the most stable Cu complex in CdTe. Due to its double-donor character, this complex causes a strong compensating effect, leading to the observed reduction of Cu doping efficiency in chlorinated CdTe.[66]

As discussed earlier, we do not expect (Te_i–Cu_{Cd}) to exist in significant amounts; yet it is another donor affecting the efficiency of Cu doping.

 This journal is © The Royal Society of Chemistry 2017

The Cu_{Cd}^{-} acceptors remaining after the association with Cl_i can be further associated with Cu_i or Cl_{Te}; the latter requires kicking out the neighbouring Te atoms by Cl during the Cu doping stage. However, taking into account the typical concentrations of Cu and Cl and the critical association energies from Fig. 4, we conclude that the association will be very weak for these defects during the high-temperature Cu doping stage. However, after the cool-down, most of the available Cu_i^{+} will be associated with the remaining Cu_{Cd}^{-} acceptors, forming the neutral (Cu_i–Cu_{Cd}) complex. Since such association does not cause additional trapping or release of free carriers, it does not influence the doping.

To visualize the predicted evolution of the defects and complexes during the Cl treatment and the Cu doping stages, we propose a flow chart shown in Fig. 5. Although not intended to quantify the concentrations of species at any particular conditions, it qualitatively shows the flows of Cl and Cu and their possible redistribution between the defects and complexes.

4.3 The recombination

The non-radiative recombination of the free carriers in CdTe absorbers is one of the most important factors limiting the resulting device performance. In this section, we discuss how the association of defects into complexes may influence non-radiative recombination of the charge carriers in CdTe absorbers and form non-uniform condition-dependent recombination profiles.

The recombination activity of a defect depends on the carrier capture rates: if capture rates are high for both electrons and holes, the recombination rate is high. Since the capture rates are determined by the electron–phonon coupling,[67–69] recombination activity of a defect could change as its electronic and phonon states change upon the association. Thus, the association and the dissociation of complexes may influence the overall carrier recombination rate.

Recent research has provided sufficient theoretical proof for the high recombination activity of the isolated Te_{Cd} defects.[24,25] However, after the Cl treatment stage known to improve the carrier lifetime in CdTe absorbers,[70–72] no isolated Te_{Cd} defects remain, because of the association with Cl_i^{-} defects (Fig. 3). Since this association changes the energies of ionization and the atomic structure of Te_{Cd}, the recombination activity of Te_{Cd} changes upon the association as well. A thorough theoretical analysis of the carrier capture rates of (Cl_i–Te_{Cd}) and (Te_i–Te_{Cd}) complexes can further clarify the role of Cl in experimentally observed lifetime improvement.

According to our calculations, some pair complexes experience strong configurational changes upon the change of the charge state. It may be the case that high recombination activity is inherent only to some particular atomic configurations of a complex. Stability of different configurations depends on the concentrations of free charge carriers[32] and, therefore, may change after changes in the external conditions (electrical bias, illumination, temperature). In addition, this means that the stability of different configurations may be spatially varied because of the non-uniform distribution of free carriers within the absorber. Therefore, it is reasonable to expect not only a non-uniform but also unstable (condition-dependent) distribution of the recombination centres within the CdTe absorber. Again, a thorough theoretical analysis of different configurations of complexes found on the right-hand-side of Fig. 5 is required to understand the challenges related to free carrier recombination in CdTe PV devices.

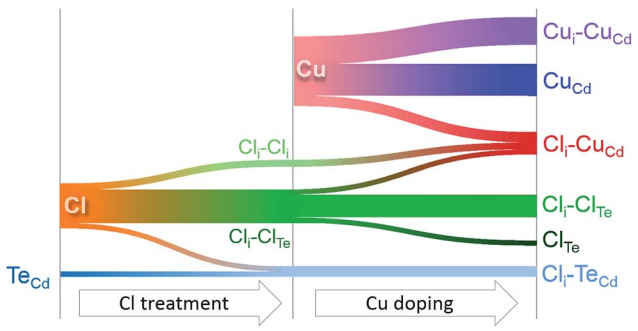

Fig. 5 Sankey diagram qualitatively showing the defect evolution during Cl treatment and Cu doping stages. Exact concentrations and flows of defects depend on experimental conditions. This particular diagram with arbitrary thicknesses of flows may or may not correspond to real conditions.

4.4 The instabilities

We define instability as a performance change on the observable time-scale after changing the ambient conditions. We also define "fast transients" as changes observable on timescales of up to 1 hour and "slow transients" as changes observable on a multihour-timescale.[44,45] In the following, we discuss the possible relation of defect association to these two types of performance transients.

Based on the available publications regarding performance transients, properties of the complexes, and instability mechanisms, we propose the following three mechanisms of instability caused by the defect association in CdTe:

- Change of atomic configuration.
- Dissociation/association of point defects.
- Diffusion mechanisms caused by the defect association.

The first mechanism belongs to a class of short-range instabilities[51] not involving the long-range diffusion of any defects. The second mechanism is also of a short-range character, but may be involved in more complex instability mechanisms along with the long-range transfer of point defects. The third mechanism is a purely long-range effect.[51]

4.4.1 The slow change of the atomic configuration. The slow change of the atomic configuration is due to the overcoming of a potential energy barrier between the atomic configurations during the change of charge state. The rate of the transition between the configurations depends on the potential barrier height and the capture rates of charge carriers. For example, the estimations made by Lany and Zunger for double-vacancy complex defects in CIGS and CIS have shown that, after turning off the light, the complex may

return to its equilibrium configuration with a time delay in the range of 100–2500 s.[32]

Therefore, slow change of atomic configuration may cause the corresponding slow changes in the doping and recombination profiles in the CdTe absorber. These effects may be responsible for some of the "fast transients" (up to one hour) after changing the conditions. The properties of (Cl_i–Cl_i), (Cl_i–Cu_{Cd}), and (Te_i–Cu_{Cd}) complexes that exhibit strong lattice relaxation are of great interest in this respect.

4.4.2 The slow association/dissociation. Any change in system conditions caused by changes in ambient temperature, illumination, or electrical bias may trigger phenomena that involve diffusion, association and dissociation of point defects and complexes. Such processes could be relatively time-consuming due to the slow diffusion of point defects, slow detachment of defects from the complex or extended defect or slow association process caused by the association energy barrier. Below, we discuss several slow mechanisms of association and dissociation of complexes in CdTe studied in this work.

The simplest case is the dissociation of weakly bound (Cl_i–Cu_{Cd}) complex with association energy of −0.40 eV caused by solar cell heating during the daily operation cycle. Our estimations show that the association degree of Cu_i may decrease from 90% to 65% upon heating from 20 to 70 °C in the case of 10^{17} cm^{-3} total Cu concentration (Fig. 6). This may cause variation in device characteristics if the complex and the isolated point defects have different properties, *e.g.*, capture cross-sections.

A more complicated example is the simultaneous change of the association degrees of several complexes after the change of conditions. For example, the binding of defects into (Cl_i–Cu_{Cd}) and (Cl_i–Cl_{Te}) complexes results from the association energies that change in the opposite way with the decrease of the Fermi level (Fig. 3). Such change in the association energies, *e.g.* during cooling, drives the system toward new equilibrium. However, chlorine redistribution between the complexes may be slow because of the slow detachment from (Cl_i–Cl_{Te}) complex or due to the slow triple-barrier diffusion of Cl_i^+ reported by Yang *et al.*[12] Furthermore, the plot of association energies in Fig. 3 suggests that the (Cl_i–Te_{Cd}) complex becomes less stable than the (Cl_i–Cu_{Cd}) when the Fermi level is low in highly p-doped material. As a result, (Cl_i–Te_{Cd}) may slowly dissociate in favour of its counterpart, exposing the Te_{Cd} recombination centre and, therefore, influencing the recombination rates in the absorber.

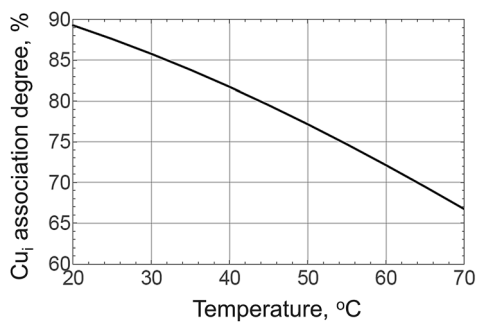

Fig. 6 The dependence of Cu_i defect association degree on temperature ($[Cu_i] = [Cu_{Cd}] = 10^{17}$ cm^{-3}).

The situation becomes even more complicated if one takes into account the changes of spatially dependent carrier generation rates and the non-equilibrium electrostatic potential. Analysis of such problems in the time-space domain would require the use of comprehensive atomistic kinetic models.

4.4.3 The slow diffusion. At least two additional diffusion mechanisms appear when we take into account the association of defects.

On the other hand, being associated with an interstitial, almost immobile[17,74] substitution defect may acquire capability to diffuse by means of the chain mechanism. Such mechanism consists of repeated kick-out of the substitution defect in the course of a chain-like process involving the interstitial–substitution pair complex and the neighbouring regular lattice atom. Predicted theoretically for the (Cl_i–Cu_{Cd}) complex, this mechanism may explain the "slow" Cu diffusion component in CdTe crystal.[11] A similar pair diffusion mechanism was proposed to explain the boron diffusion in silicon.[75] Such mechanism may facilitate the diffusion of the major substitution defects such as Cu_{Cd}, Cl_{Te}, and Te_{Cd} on the intermediate timescales between the fast diffusion of interstitial defects and the very slow direct diffusion of substitutions. In this regard, the diffusivity of (Cl_i–Cl_{Te}), (Cl_i–Te_{Cd}), and (Cl_i–Cu_{Cd}) complexes requires more study.

While the mechanism of slow configuration change plays a role mostly in the "fast transients," the second and third instability mechanisms may play an important role in the "slow" performance transients. It is hard to explain the slow transients by either the extremely slow diffusion of the substitution defects or by the very fast diffusion of the interstitial species. It was not clear how fast the diffusion of interstitials is until the recent work by Guo *et al.* showed[49] that the diffusion of isolated Cu_i^+ donors is simply too fast to explain the experimentally observed slow transient effects in the CdTe-based solar cell. Kinetic simulations performed in that work used a 1D diffusion-reaction simulator equipped with defect parameters predicted from first principles in order to study metastabilities of solar cell performance under illumination. In their simulation, the stabilization occurs within one minute as opposed to 10 hours in the corresponding experiment. This result implies that the diffusion of the interstitial defects alone cannot explain the slow transients on the multi-hour timescales. Therefore, we suggest that slow changes in defect association degree and the slow diffusion of defects may be responsible for the experimentally observed "slow transients".

4.5 Point defects *vs.* other defects

We have established that the point defects in chlorinated and Cu-doped CdTe absorbers tend to form pair complexes, and the models describing electrical properties of CdTe devices should account for this phenomenon. The question arises, however, about the applicability limits caused by other competing processes that may come into play and influence the electric behaviours. Examples of such processes are the aggregation of

 This journal is © The Royal Society of Chemistry 2017

point defects into clusters and the segregation on the extended defects. Thorough theoretical analysis of all these processes is beyond the scope of this paper, so we provide only some general comments and simple assessment of the role of different processes.

4.5.1 The large defect clusters. We assume that the formation of large defect clusters proceeds primarily *via* bimolecular reactions of the consecutive attachment of additional point defects to the most stable pair complexes. Therefore, we can assess the probability of formation of large clusters by analysing the energies of point defect attachment to the primary pair complexes. We can treat such attachment similarly to the association of two defects. For example, in order to form a triple complex, the association energy has to overcome the configuration entropy contribution separating the defects. Moreover, the association into a cluster should be more stable, as compared to the pair complexes, to be competitive. To assess the association probability of Cl- and Cu-related defects into clusters, we analyse the association of Cl_i and Cu_i defects with the most stable pair complexes, such as (Cl_i–Cl_{Te}), (Cl_i–Cl_i), (Cl_i–Cu_{Cd}), (Cl_i–Te_{Cd}), and (Cu_i–Cu_{Cd}). We find that none of the analysed cluster associations can compete with the previously analysed pair complexes in terms of stability; therefore, we would disregard these mechanisms. At the same time, we find some stable structures of $(3Te)_i$ and $(4Te)_i$ defect clusters. This means that Te_i can potentially form larger clusters, for example, under Te-rich conditions. While the properties of such clusters can be important in some cases, their formation does not influence our results on pair complex formation, and all our above conclusions hold true.

4.5.2 The segregation on extended defects. We discriminate two types of extended defects in a polycrystalline CdTe absorber with columnar grains: (i) the external grain surfaces (grain boundaries, GB) that can be highly disordered and defective and (ii) the more ordered planar (*e.g.*, twin boundaries) and line defects (*e.g.* dislocations) inside the grains. According to the available experimental data, the external GBs do not accumulate Cu,[76,77] but they do accumulate Cl.[6,65,77,78] However, Cl still penetrates the grain interior in significant concentrations from 5×10^{16} to 4×10^{17} cm^{-3}, estimated by ToF-SIMS measurements,[6,65] and may segregate on the extended defects of type (ii) inside the grain.

The most abundant extended defect of type (ii) in CdTe is $\Sigma 3$ coherent twin boundary, which has the lowest energy.[79–81] However, neither the intrinsic defects nor the Cu- or Cl-related defects segregate on such boundaries, as was shown both theoretically[12,82] and experimentally.[65] Other planar defects have much lower density than $\Sigma 3$ boundaries.

The dislocation density in CdTe usually does not exceed 10^5 to 10^6 cm^{-2}.[79,83] Even if packed with the point defects very tightly, dislocations can accommodate only up to 10^{14} cm^{-3} point defects, *i.e.*, 3–4 orders of magnitude less than the overall density of Cu and Cl elements in the grain interior. Therefore, we conclude that while some amount of Cl and Cu atoms can segregate on the extended defects of type (ii), most of the intragrain Cu and Cl atoms reside in point defects and pair defect complexes.

5. Conclusions and outlook

We have analysed the thermodynamic aspects of defect interactions in Cl- and Cu-treated CdTe absorbers using first-principles calculations. Below, we list the most important findings made in this work:

- There exists a number of pair complexes with negative association enthalpy, including some donor–donor complexes.
- The interstitial–vacancy complexes and the complexes formed by self-interstitial with substitution defect are unstable.
- There are several complexes with strong lattice relaxation.
- Interstitial Cl defects (Cl_i) participate in the formation of the most favourable complexes.
- All the primary pair complexes in p-type CdTe exhibit either neutral or donor character.

We have identified several pair complexes that could be present in CdTe absorbers and may influence device performance and stability. While only the detailed kinetic simulations of the cell preparation and field operation may reveal the actual role of defect association, we can still derive general conclusions about the role of the most important complexes in CdTe.

The most tightly bound complexes in chlorinated CdTe are those associating the Te_{Cd} antisite defect: (Cl_i–Te_{Cd}) and (Te_i–Te_{Cd}). If association in stable complexes indeed passivates Te_{Cd} recombination centres, it would explain the role of Cl treatment in the improvement of free carrier lifetime in CdTe. The neutral (Cl_i–Cl_{Te}) complexes are presumably the most abundant in chlorinated CdTe absorbers before Cu treatment. After Cu introduction and activation, (Cl_i–Cl_{Te}) complexes dissociate in favour of more stable $(Cl_i–Cu_{Cd})^{2+}$ complexes that become the dominant compensating defects limiting the p-type doping. On the cool-down, Cu_{Cd}^- acceptors formed during Cu annealing tend to bind available Cu_i^+ interstitials to form neutral (Cu_i–Cu_{Cd}) complexes that do not influence the doping.

Association of the point defects into pair complexes may introduce several mechanisms for the instabilities, including:

- Slow change of the atomic configuration of the complexes with the large lattice relaxation.
- Slow dissociation/association of point defects, and.
- Slow diffusion mechanisms caused by the defect association.

The latter two mechanisms may play an important role in the performance changes observed on the multi-hour timescale. To further clarify these effects, the kinetic parameters are needed for several complexes, including (Cl_i–Cl_{Te}), (Cl_i–Te_{Cd}), (Cl_i–Cu_{Cd}), and (Cu_i–Cu_{Cd}) complexes. Required parameters include the carrier capture rates, diffusivities, and the barriers for changing the atomic configuration and association/dissociation.

According to our calculations, large cluster complexes involving Cl and Cu in the bulk of CdTe grains are less favourable energetically as compared to pair complexes. At the same time, the large clusters of Te_i may form under some conditions, and deserve further investigation.

Acknowledgements

We thank Andrei Los and Marcus Gloeckler for the helpful discussions.

References

1 Best Research-Cell Efficiencies, National Renewable Energy Laboratory, http://nrel.gov/ncpv/images/efficiency_chart.jpg.
2 J. M. Burst, J. N. Duenow, D. S. Albin, E. Colegrove, M. O. Reese, J. A. Aguiar, C.-S. Jiang, M. K. Patel, M. M. Al-Jassim, D. Kuciauskas, S. Swain, T. Ablekim, K. G. Lynn and W. K. Metzger, *Nature Energy*, 2016, **1**, 16015.
3 S. G. Kumar and K. S. R. Koteswara Rao, *Energy Environ. Sci.*, 2014, **7**, 45.
4 V. Evani, M. Khan, S. Collins, V. Palekis, P. Bane, D. Morel and C. Ferekides, *Photovoltaic Specialist Conference (PVSC), IEEE 42nd*, New Orleans, LA, 2015, DOI: 10.1109/PVSC.2015.7356098.
5 T. A. Gessert, W. K. Metzger, P. Dippo, S. E. Asher, R. G. Dhere and M. R. Young, *Thin Solid Films*, 2009, **517**, 2370–2373.
6 S. P. Harvey, G. Teeter, H. Moutinho and M. M. Al-Jassim, *Prog. Photovoltaics*, 2015, **23**, 838–846.
7 J. Perrenoud, L. Kranz, C. Gretener, F. Pianezzi, S. Nishiwaki, S. Buecheler and A. N. Tiwari, *J. Appl. Phys.*, 2013, **114**, 174505.
8 N. E. Gorji, *Appl. Phys. A: Mater. Sci. Process.*, 2015, **119**, 275–284.
9 J. Ma, S.-H. Wei, T. A. Gessert and K. K. Chin, *Phys. Rev. B: Condens. Matter Mater. Phys.*, 2011, **83**, 245207.
10 J.-H. Yang, W.-J. Yin, J.-S. Park, W. Metzger and S.-H. Wei, *J. Appl. Phys.*, 2016, **119**, 045104.
11 D. Krasikov, A. Knizhnik, B. Potapkin, S. Selezneva and T. Sommerer, *Thin Solid Films*, 2013, **535**, 322–325.
12 J.-H. Yang, W.-J. Yin, J.-S. Park, J. Ma and S.-H. Wei, *Semicond. Sci. Technol.*, 2016, **31**, 083002.
13 S.-H. Wei and S. B. Zhang, *Phys. Rev. B: Condens. Matter Mater. Phys.*, 2002, **66**, 155211.
14 J.-H. Yang, J.-S. Park, J. Kang, W. Metzger, T. Barnes and S.-H. Wei, *Phys. Rev. B: Condens. Matter Mater. Phys.*, 2014, **90**, 245202.
15 S. Lany, V. Ostheimer, H. Wolf and Th. Wichert, *Phys. B*, 2001, **308–310**, 958–962.
16 M.-H. Du, H. Takenaka and D. J. Singh, *J. Appl. Phys.*, 2008, **104**, 093521.
17 V. Lordi, *J. Cryst. Growth*, 2013, **379**, 84–92.
18 R. Grill and A. Zappettini, *Prog. Cryst. Growth Charact. Mater.*, 2004, **48/49**, 209–244.
19 R. Grill, B. Nahlovskyy, E. Belas, M. Bugar, P. Moravec and P. Hoschl, *Semicond. Sci. Technol.*, 2010, **25**, 045019.
20 K. Biswas and M.-H. Du, *New J. Phys.*, 2012, **14**, 063020.
21 D. Krasikov, A. Knizhnik, B. Potapkin and T. Sommerer, *MRS Online Proc. Libr.*, 2014, **1638**, DOI: 10.1557/opl.2014.148.
22 A. Lindström, S. Mirbt, B. Sanyal and M. Klintenberg, *J. Phys. D: Appl. Phys.*, 2016, **49**, 035101.
23 A. Lindström, M. Klintenberg, B. Sanyal and S. Mirbt, *AIP Adv.*, 2015, **5**, 087101.
24 D. N. Krasikov, A. V. Scherbinin, A. A. Knizhnik, A. N. Vasiliev, B. V. Potapkin and T. J. Sommerer, *J. Appl. Phys.*, 2016, **119**, 085706.
25 J.-H. Yang, L. Shi, L.-W. Wang and S.-H. Wei, *Sci. Rep.*, 2016, **6**, 21712.
26 A. Carvalho, S. Öberg and P. R. Briddon, *Thin Solid Films*, 2011, **519**, 7468.
27 A. Garcia and J. E. Northrup, *Phys. Rev. Lett.*, 1995, **74**, 1131–1134.
28 Y. Ke, S. Lany, J. J. Berry, J. D. Perkins, P. A. Parilla, A. Zakutayev, T. Ohno, R. O'Hayre and D. S. Ginley, *Adv. Funct. Mater.*, 2014, **24**, 2875–2882.
29 P. Erhart, P. Traskelin and K. Albe, *Phys. Rev. B: Condens. Matter Mater. Phys.*, 2013, **88**, 024107.
30 D. O. Demchenko, I. C. Diallo and M. A. Reshchikov, *Phys. Rev. Lett.*, 2013, **110**, 087404.
31 C. E. Dreyer, A. Alkauskas, J. L. Lyons, J. S. Speck and C. G. Van de Walle, *Appl. Phys. Lett.*, 2016, **108**, 141101.
32 S. Lany and A. Zunger, *J. Appl. Phys.*, 2006, **100**, 113725.
33 K. Decock, P. Zabierowski and M. Burgelman, *J. Appl. Phys.*, 2012, **111**, 043703.
34 K. Macielak, M. Maciaszek, M. Igalson, P. Zabierowski and N. Barreau, *IEEE Journal of Photovoltaics*, 2015, **5**, 1206–1211.
35 S. M. Myers, M. I. Baskes, H. K. Birnbaum, J. W. Corbett, G. G. DeLeo, S. K. Estreicher, E. E. Haller, P. Jena, N. M. Johnson, R. Kirchheim, S. J. Pearton and M. J. Stavola, *Rev. Mod. Phys.*, 1992, **64**, 559.
36 T. Tanabe, *Phys. Scr.*, 2014, **159**, 014044.
37 C. Freysoldt, B. Grabowski, T. Hickel and J. Neugebauer, *Rev. Mod. Phys.*, 2014, **86**, 253–305.
38 K. D. Dobson, I. Visoly-Fisher, G. Hodes and D. Cahen, *Sol. Energy Mater. Sol. Cells*, 2000, **62**, 295–325.
39 S. Erra, C. Shivakumar, H. Zhao, K. Barri, D. L. Morel and C. S. Ferekides, *Thin Solid Films*, 2007, **515**, 5833–5836.
40 C. Deline, J. del Cueto, D. S. Albin and S. Rummel, *J. Photonics Energy*, 2012, **2**(1), 022001.
41 S. B. Schujman, J. R. Mann, C. Hull, A. Conteh, G. Dufresne, L. M. LaQue, C. Rice, D. Taylor, J. Wax, D. J. Metacarpa and P. Haldar, *Photovoltaic Specialist Conference (PVSC), IEEE 40th*, Denver, CO, June 2014, pp. 2626–2629.
42 C. Gretener, J. Perrenoud, L. Kranz, E. Cheah, M. Dietrich, S. Buecheler and A. N. Tiwari, *Sol. Energy Mater. Sol. Cells*, 2016, **146**, 51–57.
43 I. Rimmaudo, A. Salavei, B. L. Xu, S. Di Mare and A. Romeo, *Thin Solid Films*, 2015, **582**, 105–109.
44 C. Deline, J. del Cueto, D. S. Albin, C. Petersen, L. Tyler and G. TamizhMani, *Photovoltaic Specialists Conference (PVSC), 2011, IEEE 37th*, Seattle, WA, June 2011, pp. 003113–003118.
45 T. J. Silverman, M. G. Deceglie, B. Marion and S. R. Kurtz, *Photovoltaic Specialist Conference (PVSC), 2014, IEEE 40th*, Denver, CO, June 2014, pp. 3676–3681.
46 M. Gostein and L. Dunn, *Photovoltaic Specialists Conference (PVSC), 2011, IEEE 37th*, Seattle, WA, June 2011, pp. 003126–003131.

 This journal is © The Royal Society of Chemistry 2017

47 M. Nardone and D. Albin, *IEEE Journal of Photovoltaics*, 2015, **8**, 962.
48 D. Guo, R. Akis, D. Brinkman, A. Moore. T. Fang, I. Sankin, D. Vasileska and C. Ringhofer, *Photovoltaic Specialist Conference (PVSC), IEEE 42nd*, New Orleans, LA, June 2015, pp. 1–5.
49 D. Guo and D. Vasileska, *2016 International Conference on Numerical Simulation of Optoelectronic Devices (NUSOD)*, Sydney, NSW, 2016, pp. 181–182, DOI: 10.1109/NUSOD 2016.7547094.
50 N. Abdollahi and N. E. Gorji, *Superlattices Microstruct.*, 2016, **100**, 9.
51 J.-F. Guillemoles, L. Kronik, D. Cahen, U. Rau, A. Jasenek and H.-W. Schock, *J. Phys. Chem. B*, 2000, **104**, 4849.
52 T. Mattila and A. Zunger, *Phys. Rev. B: Condens. Matter Mater. Phys.*, 1998, **58**, 1367.
53 P. E. Blöchl, *Phys. Rev. B: Condens. Matter Mater. Phys.*, 2000, **62**, 6158.
54 G. Kresse and J. Furthmuller, *Phys. Rev. B: Condens. Matter Mater. Phys.*, 1996, **54**, 11169.
55 *MedeA® version 2.19*, Materials Design Inc., Angel Fire, New Mexico, USA, 2011.
56 P. E. Blöchl, *Phys. Rev. B: Condens. Matter Mater. Phys.*, 1994, **50**, 17953.
57 G. Kresse and D. Joubert, *Phys. Rev. B: Condens. Matter Mater. Phys.*, 1999, **59**, 1758.
58 J. P. Perdew, K. Burke and M. Ernzerhof, *Phys. Rev. Lett.*, 1996, **77**, 3865.
59 J. Heyd, G. E. Scuseria and M. Ernzerhof, *J. Chem. Phys.*, 2006, **118**, 8207.
60 C. G. Van de Walle, *J. Appl. Phys.*, 2004, **95**, 3851–3879.
61 J.-H. Yang, J.-S. Park, J. Kang and S.-H. Wei, *Phys. Rev. B: Condens. Matter Mater. Phys.*, 2015, **91**, 075202.
62 J. L. Roehl and S. V. Khare, *Sol Energ*, 2014, **101**, 245–253.
63 K. Alberi and M. A. Scarpulla, *Sci. Rep.*, 2016, **6**, 27954.
64 D. Krasikov, A. Knizhnik, B. Potapkin and T. Sommerer, *Semicond. Sci. Technol.*, 2013, **28**, 125019.
65 D. Mao, C. E. Wickersham Jr and M. Gloeckler, *IEEE Journal of Photovoltaics*, 2014, **4**, 1655.
66 S. A. Jensen, J. M. Burst, J. N. Duenow, H. L. Guthrey, J. Moseley, H. R. Moutinho, S. W. Johnston, A. Kanevce, M. M. Al-Jassim and W. K. Metzger, *Appl. Phys. Lett.*, 2016, **108**, 263903.
67 A. Alkauskas, Q. Yan and C. G. Van de Walle, *Phys. Rev. B: Condens. Matter Mater. Phys.*, 2014, **90**, 075202.
68 L. Shi, K. Xu and L.-W. Wang, *Phys. Rev. B: Condens. Matter Mater. Phys.*, 2015, **91**, 205315.
69 G. D. Barmparis, Y. S. Puzyrev, X.-G. Zhang and S. T. Pantelides, *Phys. Rev. B: Condens. Matter Mater. Phys.*, 2015, **92**, 214111.
70 H. R. Moutinho, M. M. Al-Jassim, D. H. Levi, P. C. Dippo and L. L. Kazmerski, *J. Vac. Sci. Technol., A*, 1998, **16**, 1251.
71 W. K. Metzger, D. Albin, M. J. Romero, P. Dippo and M. Young, *J. Appl. Phys.*, 2006, **99**, 103703.
72 L. Kranz, C. Gretener, J. Perrenoud, D. Jaeger, S. S. A. Gerstl, R. Schmitt, S. Buecheler and A. N. Tiwari, *Adv. Energy Mater.*, 2014, **4**, 1301400.
73 R. A. Oriani, *Acta Metall.*, 1970, **18**, 147–157.
74 E. Colegrove, S. P. Harvey, J.-H. Yang, J. M. Burst, D. S. Albin, S.-H. Wei and W. K. Metzger, *Phys. Rev. Appl.*, 2016, **5**, 054014.
75 W. Windl, M. M. Bunea, R. Stumpf, S. T. Dunham and M. P. Masquelier, *Phys. Rev. Lett.*, 1999, **83**, 4345.
76 D. Mao, G. Blatz, C. E. Wickersham Jr and M. Gloeckler, *Sol. Energy Mater. Sol. Cells*, 2016, **157**, 65.
77 J. D. Major, *Semicond. Sci. Technol.*, 2016, **31**, 093001.
78 J. D. Poplawsky, C. Li, N. R. Paudel, W. Guo, Y. Yan and S. J. Pennycook, *Sol. Energy Mater. Sol. Cells*, 2016, **150**, 95–101.
79 K. Durose in *CdTe and Related Compounds, Physics, Defects, Hetero- and Nano-structures, Crystal Growth, Surfaces and Applications: Part II: Crystal Growth, Surfaces and Applications*, ed. R. Triboulet and P. Siffert, Elsevier, Amsterdam, 2010, pp. 4–18.
80 J.-S. Park, J. Kang, J.-H. Yang, W. Metzger and S.-H. Wei, *New J. Phys.*, 2015, **17**, 013027.
81 Y. Yan, M. M. Al-Jassim and T. Demuth, *J. Appl. Phys.*, 2001, **90**, 3952.
82 C. Buurma, T. Paulauskas, Z. Guo, R. Klie and M. K. Y. Chan, *Microsc. Microanal.*, 2014, **20**(S3), 528.
83 K. N. Zaunbrecher, D. Kuciauskas, C. H. Swartz, P. Dippo, M. Edirisooriya, O. S. Ogedengbe, S. Sohal, B. L. Hancock, E. G. LeBlanc, P. A. R. D. Jayathilaka, T. M. Barnes and T. H. Myers, *Appl. Phys. Lett.*, 2016, **109**, 091904.

View publication stats